Supplementary Information

Photoresponse of Graphene Channel in Graphene-Oxide-Silicon Photodetectors

Kuo-Chih Lee[1], Yu-Hsien Chuang[2], Chen-Kai Huang[1], Hui Li[1], Guo-En Chang[3], Kuan-Ming. Hung[4], Hung Hsiang Cheng[1]

1. Center for Condensed Matter Sciences and Graduate Institute of Electronics Engineering, National Taiwan University, Taipei 106, Taiwan
2. Graduate School of Advanced Technology Program for Semiconductor Devices, Materials, and Hetero-integration, National Taiwan University, Taipei 106, Taiwan
3. Department of Mechanical Engineering, and Advanced Institute of Manufacturing with High-tech Innovations, National Chung Cheng University, Chiayi County 62102, Taiwan
4. Department of Electronics Engineering, National Kaohsiung University of Science and Technology, Kaohsiung 807, Taiwan

Contents:

S1. Device fabrication process, TEM characterization on oxide thickness, SEM characterization on device, Raman examination on the formation of graphene on SiO_2/Si, and photocurrent measurement

The device was fabricated in three steps. (a) First, a thin SiO_2 layer was grown on n-type Si wafer with a resistance of 5 Ohm-cm at a temperature of 400°C in the presence of a dry oxygen flow at atmospheric pressure. (b) Two rectangle metal pads (made of 50-nm-Ti/120-nm-Au) were then deposited on top of the SiO_2 layer with a separation of 0.5 mm. (c) Graphene layer was thereafter transferred to the top of the sample through a wet transfer process.

Prior to the transfer of graphene onto the SiO_2/Si sample, the layer thickness of deposited SiO_2 was characterized by high-resolution transmission electron microscopy (HRTEM, JEOL model 2100F), as depicted in Figure S1. (In the HRXTEM measurements, a thin metal was deposited on the surface of the film by Atomic Layer Deposition to reveal the contrast of the oxide layer. The measurements were performed at Msscorps Co., LTD, Taiwan.) The oxide layer was measured as (d_{ox}) 27 ± 2 Å, indicated by the red ellipsoidal region-of-interest in Figure S1.

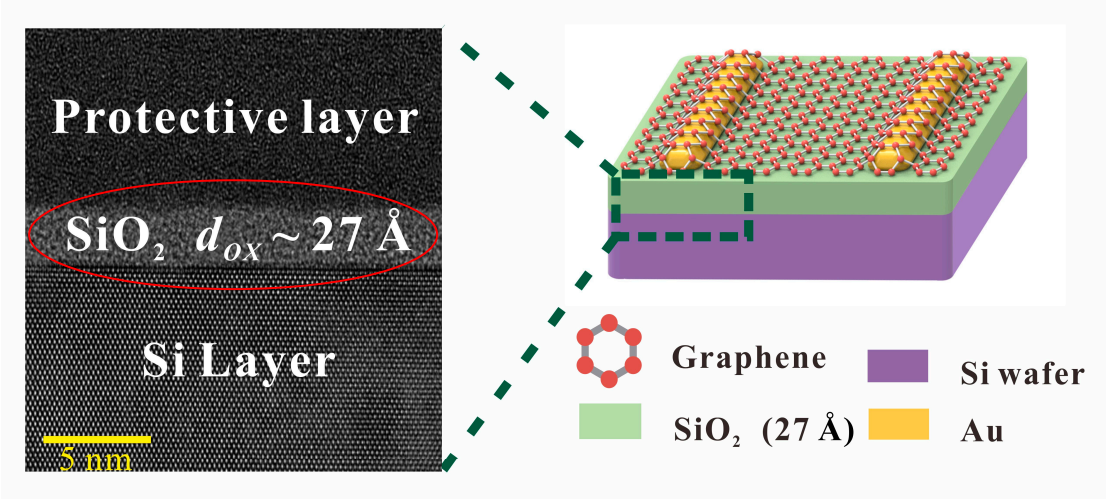

Figure S1. High-resolution cross-sectional electron microscopy image of the as-grown SiO_2/Si sample; the layer thickness of the SiO_2 layer is d_{OX} = 27 Å ± 2 Å.

In addition to the TEM characterization, Field Emission Scanning Electron Microscope (FESEM) measurement was also performed. (Model Hitachi 8220) Figure S2 a. shows the top view of the device where two metal pads are used for the current-voltage measurement and the channel area are clearly resolved. Separation between the two metal pads is 0.5 mm. Figure S2 b. shows the cross-sectional view focus at the edge of the metal pad where a clear layer (SiO_2) is revealed as marked by the red circles. Figure S2c. presents a cross-sectional view focused on SiO_2/Si. The layer contrast between SiO_2/Si is not as evident as that in the TEM image. Thus, the

oxide layer thickness was determined based on the TEM image.

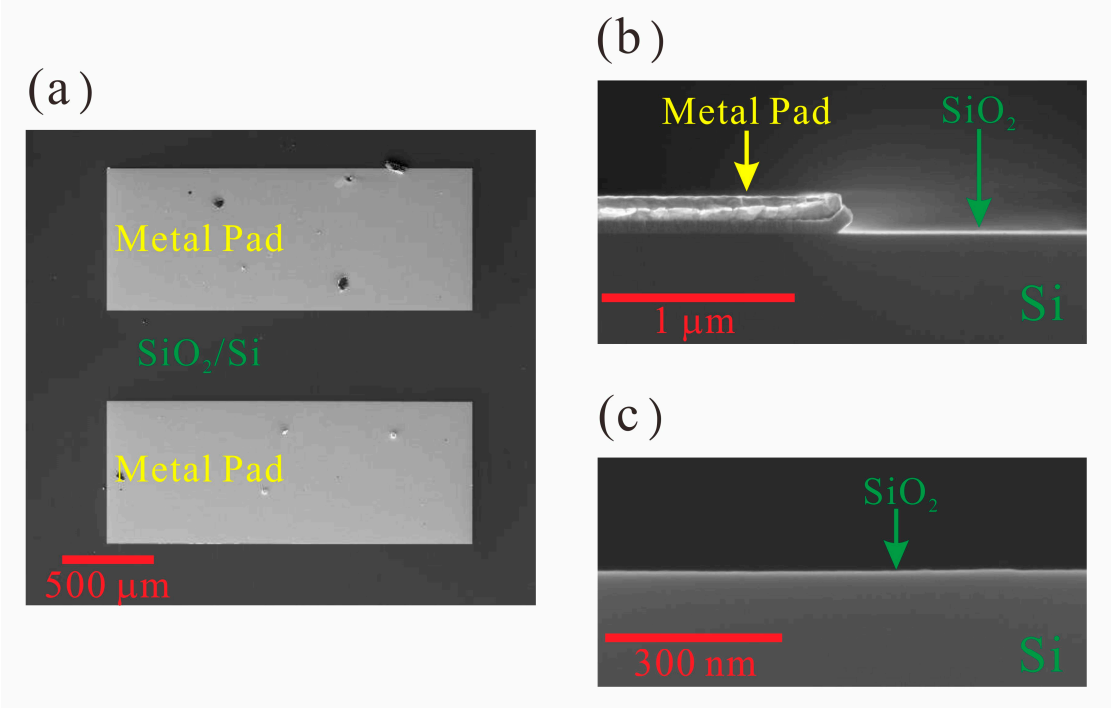

Figure S2 Field Emission Scanning Electron Microscope image of the device.

Transferring process of graphene onto SiO_2/Si

Graphene purchased from ACS material (ACS Material Trivial Transfer Graphene [32]) was used in the fabrication, and the monolayer was transferred to the surface of SiO_2/Si via a wet transfer process. Schematic representation of the transfer processes is shown in Figure S3.

(a) The monolayer graphene shipped from the company comprised two protective layers of polymethylmethacrylate (PMMA) and a polydimethylsiloxane (polymer) layer, as illustrated in Figure S3a.

(b) The sample was placed in DI water ($R \approx 18\ M\Omega$) to remove the polymer layer (Figure S3 b).

(c) The sample of SiO_2/Si and graphene was placed in DI water (Figure S3 c).

(d) The finished sample was placed in a vacuum chamber for 1 h to remove water from the surface (Figure S3d).

(e) The sample (PMMA/Graphene/SiO_2/Si) was placed in dilute acetone to remove PMMA (Figure S3e).

(f) After rinsing off PMMA, the sample was cleaned with DI water and dried with nitrogen gas (Figure S3f).

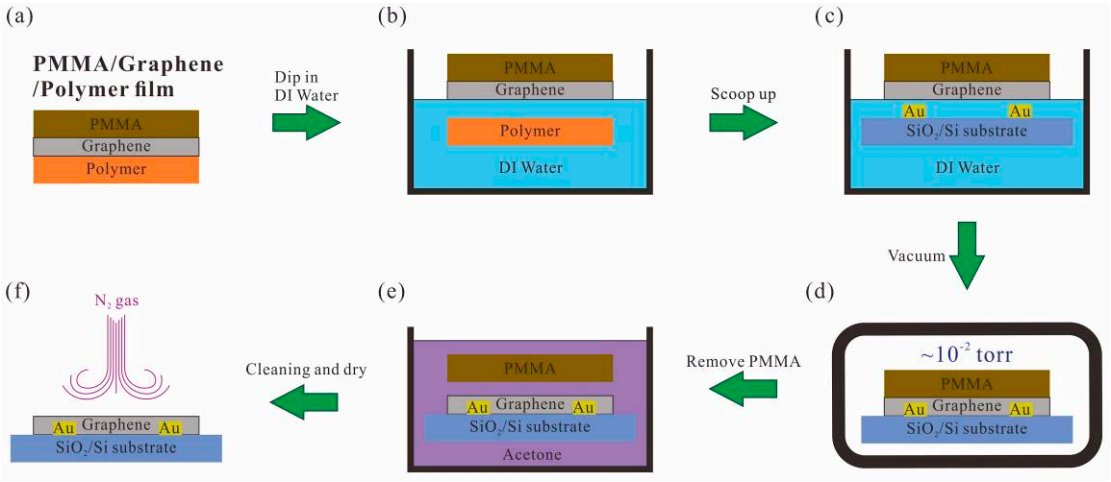

Figure S3 Schematic representation of the transfer processes.

Raman examination on the formation of graphene on SiO_2/Si

Raman measurement was performed to examine the formation of graphene on SiO_2/Si using 532 nm laser. The spectrum is depicted in Figure S4. Two main features are resolved located at 1579 cm^{-1} (G peak) and 2708 cm^{-1} (2D peak) as marked by the arrow line and the Raman intensity of 2D peak is larger than the G peak. These two features reflect the successful fabrication of single-layer graphene on SiO_2/Si and the details have been discussed in the literature, taken from reference 33 and 34.

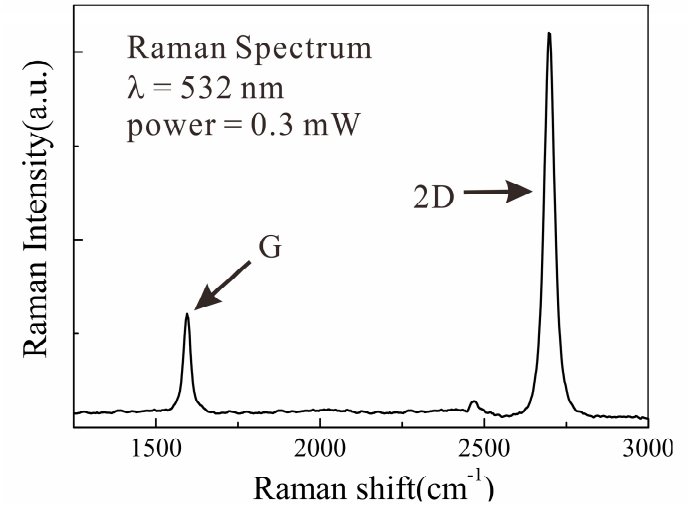

Figure S4 Raman spectrum of the device focused in the range of graphene.

Photocurrent measurement

Photocurrent measurement was conducted by using AC detection scheme. A mechanical chopper was placed in front of the sample operated at a frequency of 98 Hz and the photoresponse of the device was recorded by lock-in amplifier (SRS, SR830). (The lock-in amplifier was operated with a frequency set to the chopper frequency to filter the noise.) It gives a value corresponding to the difference between the current in dark and under illumination. The dark current is associated with the intrinsic p-type carrier while the photocurrent (current under illumination) consists the current induced by photogating effect in addition to dark current. Thus, the current induced by photogating effect is revealed. For operating the device with back-gate bias, a DC voltage source (SR570) was used.

The photocurrent was also recorded by DC measurement. A temporal photocurrent curve under light-on and light-off conditions obtained via DC measurements is depicted in Figure S5. The difference between light-on and light-off current is approximately 2.6 μA, which is consistent with the result of AC measurement presented in the manuscript.

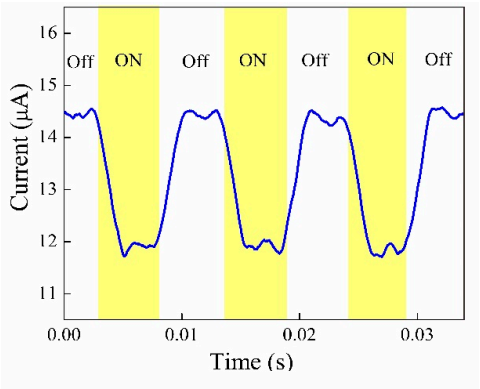

Figure S5. Temporal photocurrent curve under light-on and light-off conditions obtained via DC measurements.

S2. Equilibrium energy profile described in details

The energy profile of the system was established by lining the Fermi levels of the three layers. The Fermi energy of the Si film was determined by $E_F = E_C - k_B T ln(N_C/N_D)$, where E_C denotes the energy of the Si conduction-band edge with respect to the valence-band edge E_V, k_B is the Boltzmann constant, N_C is the effective density of states in the conduction band, and N_D is the doping concentration in the Si film. The Fermi level was found to be 0.855 eV above the valence-band edge. The approximate amount of band bending at the oxide/Si interface was evaluated as $\approx q\,\phi_g - q\chi_{Si} - E_c + E_F$, where χ_g denotes the intrinsic work function of graphene and χ_{Si} is the Si affinity. In modeling band bending and the energy offset between the layers, $q\chi_g = 4.89\ \text{eV}$, $q\chi_{SiO_2} = 0.9\ \text{eV}$, and $q\chi_{Si} = 4.05\ \text{eV}$ were used in the calculation [35].

S3. Resistance behavior of other devices

Three devices were fabricated from three samples cut from the same Si wafer with dimensions of 2 cm × 2 cm. These three 2 cm × 2 cm samples were independently fabricated into graphene/SiO_2/Si using the same procedure described above. The resistance of the graphene channel of device 1 under back-gated bias is shown in Figure 2a in the manuscript. The result for device 2 is depicted in S6, exhibiting an R characteristic similar to that of device 1. A critical voltage of 1.05 V was obtained, which is a small deviation of 5% compared to that of device 1.

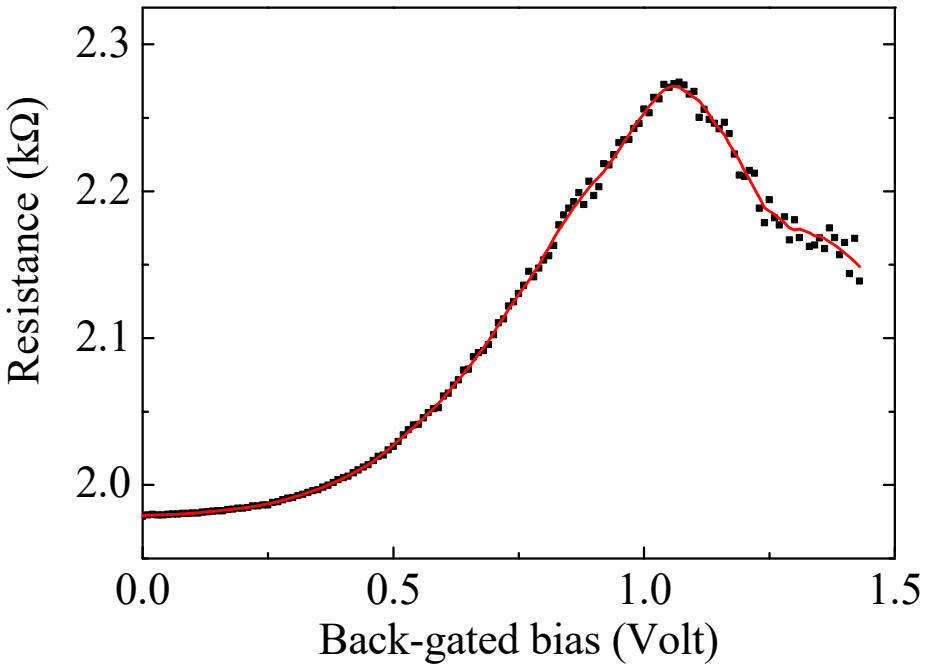

Figure S6. Resistance of the graphene layer of device 2 plotted as a function of back-gated bias.

S4. Hole mobility of graphene channel

The hole mobility in the graphene channel was estimated using transconductance measurements [36]. The current of the channel (I_{Gra}) was recorded at a fixed voltage (0.1 V) applied across the two metal contacts on the graphene with different back-gated biases (V_{BG}). The results are depicted in Figure S7. The mobility can then be estimated as $\mu = \frac{1}{C_g}\frac{L}{W}\left(\frac{\Delta I_{Gra}}{\Delta V_{BG}}\right)\frac{1}{V_{DS}}$, where C_g denotes the capacitance of the oxide layer. Taking C_g = 1.28 X 10^{-6} F/cm^2 and L/W = 4, the mobility of graphene was found to be 100 cm^2/V-s.

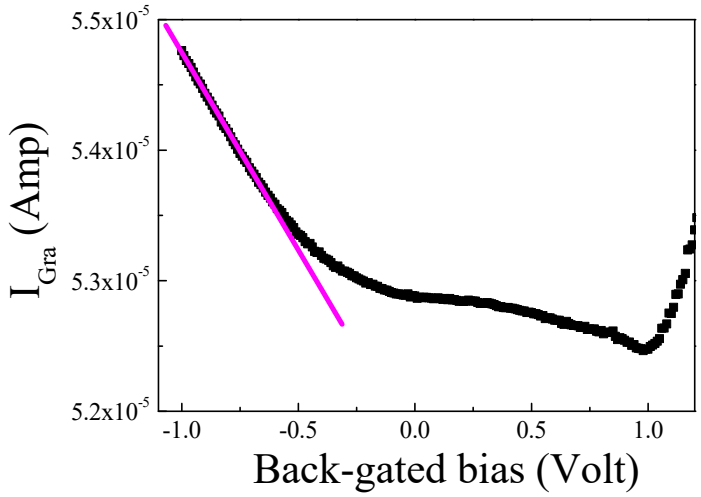

Figure S7. Meaured current of the graphene layer at various gate biases.

S5. Photocurrent measurement with laser wavelengths of 808 and 633 nm

Photocurrent measurements were also performed with two other laser wavelengths of laser power of 808 and 633 nm at a power of 0.26 W/cm^{-2}. Photocurrents of 2.2 and 1.97 μA are recorded for laser wavelengths of 808 and 633 nm, respectively, corresponding to carrier concentrations of 1.15 and 1.03 × 10^{12} cm^{-2} with the same order of magnitude as that of a laser wavelength of 1064 nm [37]. Figure S8 depicts the photocurrent under bias at laser wavelengths of 808 and 633 nm. Decrease-to-increase characteristic is also observed as that of a laser wavelength of 808 and 633 nm illustrated.

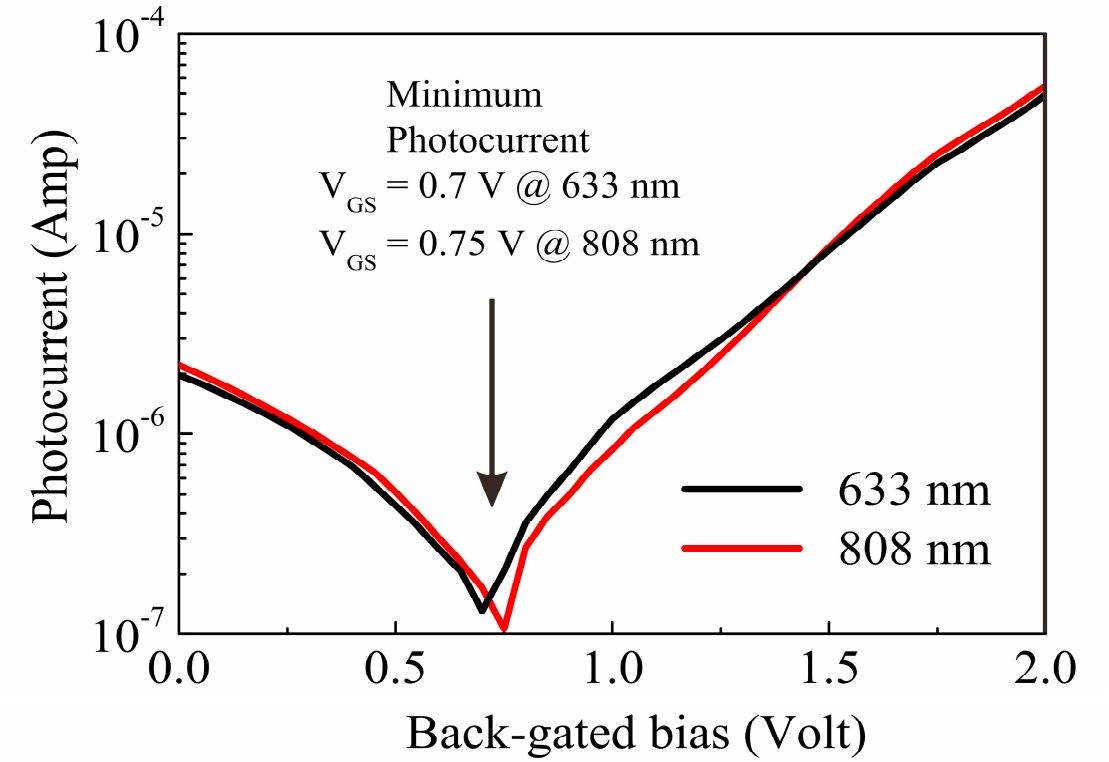

Figure S8. The bias voltage dependent photocurrent characteristics with different wavelength.